Catechol Derivative RAFT Agent for Surface Functionalization of Magnetic Nanoparticles

Serkan Demirci

Department of Chemistry, Amasya University, Amasya 05100 Turkey
+90 358 2421614, sdemirci@amasya.edu.tr

Received: 27th April 2016
Accepted: 18th November 2016
DOI: http://dx.doi.org/10.18466/cbujos.302636

Abstract

Functional nanoparticles (NPs), Fe_3O_4@SiO_2-PMEMA, were prepared via surface initiated reversible addition-fragmentation chain transfer (RAFT) polymerization, using catechol-based biomimetic RAFT agent incorporating a trithiocarbonate unit and 2-*N*-morpholinoethyl methacrylate (MEMA) as the monomer. Poly(2-*N*-morpholinoethyl methacrylate) (PMEMA) were synthesized on biomimetic RAFT agent functionalized Fe_3O_4@SiO_2 NPs surface. The prepared NPs were characterized at the different modification stages using attenuated total reflectance-Fourier transform infrared spectroscopy (FTIR), X-ray photoelectron spectroscopy (XPS), X-ray diffraction (XRD), thermogravimetric analysis (TGA) and transmission electron microscope (TEM). The magnetic properties of NPs were also determined by vibrating sample magnetometer (VSM).

Keywords — Biomimetic, catechol derivatives, magnetic nanoparticles, RAFT polymerization

1 Introduction

Over the years, magnetic polymeric nanoparticles with sizes ranging from several to ~20 nm have been received more attention because of the application of magnetism to varied area, such as biomedical [1-7], environment and food analyses [8], and industrial water treatment [9].

Surface functionalization is one of the most effective methods for preparing polymer coated NPs. Mostly, two approaches are employed to functionalize NPs: "grafting from" and "grafting to". There are two main advantages of the "grafting from" technique. First, homogeneous polymer layers can be prepared. Second, this technique gives relatively high grafting densities [10-12]. The attachment of ticker polymer chains to NPs surface was achieved via combination of "grafting from" and controlled radical polymerization techniques including nitroxide-mediated radical polymerization (NMP) [13], single electron transfer-living radical polymerization (SET-LRP) [14], atom transfer radical polymerization (ATRP) [15-16] and reversible addition-fragmentation chain transfer (RAFT) polymerization [17-19].

Attached initiating groups initiate the surface-initiated polymerization from the surface [20-23]. The surface immobilized RAFT agent has become the other option for modified the surface via surface-initiated RAFT polymerization [24-26]. The RAFT agent and/or initiator can be attached on solid subtract via variety of strategies such as self-assembly monolayers, click chemistry, catechol and etc [19,27-29]. Recently, catechol derivatives have emerged major attention for the functionalization of various surfaces.

Zobrist et al [30]. demonstrated a novel strategy for polymer modified titanium surface with dopamine functionalized polymers chains. The monomers were polymerized in the presence of the catechol derivative RAFT agent. These polymers were immobilized on titanium surface. Liu et al [28]. reported the synthesis of a novel ionic liquid containing a biomimetic cate-

cholic functional group, and immobilized onto silicon surface for allowing the tribological protection. The synthesis of poly(styrene) brushes using catechol-functional RAFT agent was described by Liu et al [29]. Polymer brushes were generated via combination of "grafting from" and "grafting to" methodologies. Compared with the polymer brushes were generated via "grafting to" approach, the polymer brushes created "grafting from" methodology were much denser and more homogeneous.

Herein, PMEMA functionalized Fe_3O_4 NPs were successfully produced by surface initiated RAFT polymerization with the goal of fabricating multi-functional NPs. The morphological characterization of MNPs was carried out by using transmission electron microscopy (TEM). The other characteristics of the MNPs were investigated by attenuated total reflectance-Fourier transform infrared spectroscopy (FTIR), X-ray photoelectron spectroscopy (XPS), X-ray diffraction (XRD), thermogravimetric analysis (TGA) and vibrating sample magnetometer (VSM).

2 Experimental

2.1 Materials

2-*N*-Morpholinoethyl methacrylate (MEMA, 95%), iron(II) chloride tetrahydrate ($FeCl_2.4H_2O$, ≥99%), iron(III) chloride hexahydrate ($FeCl_3.6H2O$, 97%), tetraethyl orthosilicate (TEOS, ≥99%), dopamine hydrochloride (DA, 99%), 4-cyano-4-(phenylcarbonothioylthio)pentanoic acid (CPAD, >97%), *N*-hydroxysuccinimide (NHS, 98%), *N*-methyl-2-pyrrolidone (NMP, 99.5%), *N,N'*-dicyclohexylcarbodiimide (DCC, 99%), triethylamine (TEA, ≥99%), magnesium sulfate ($MgSO_4$, ≥99.5%), 2,2'-azobis(2-methylpropionitrile) (AIBN, 98%), dichloromethane (DCM, anhydrous), tetrahydrofuran (THF, ≥99.9%), *n*-hexane (≥95%), ammonium hydroxide solution (28 wt%, NH_3 in H_2O) were purchased commercially from Sigma-Aldrich and used as purchased unless otherwise specified. The water was used from a Millipore Milli-Q ultrapure water system.

2.2 Synthesis of Catechol Derivative RAFT Agent

The synthesis of catechol derivative RAFT agent was performed following the reported method [28]. ^{1}H NMR (300 MHz, $CDCl_3$, ppm) δ: 7.8-8.1 (d, 1H, CH-C), 7.4-7.6 (t, 1H, CH-CH), 7.4-7.5 (t, 2H, CH-CH), 6.8-6.9 (d, 1H, C-CH-CH), 6.7-6.8 (s, 1H, C-CH-C), 6.7-6.8 (d, 1H, CH-CH-C-OH), 5.9-6.0 (s, NH), 3.5-3.6 (t, 2H, CH_2-CO), 2.5-2.7 (t, CH_2-NH), 2.4-2.6 (m, 1H, CH_2-C), 2.46-2.48 (m, 2H, CH_2-C-C), 2.34-2.41 (m, 1H, CH_2-C), 1.88 (s, 3H, CH_3).

2.3 Synthesis of Poly[2-(*N*-morpholino)ethyl methacrylate] (PMEMA) modified NPs

Fe_3O_4 nanoparticles were synthesized as reported in the literature [31]. Fe_3O_4@SiO_2 NPs first treated with piranha solution for 1h, washed thoroughly with water and dried. The Fe_3O_4@SiO_2 NPs were then immersed in a 1.0 mM acetone solution of catechol derivative RAFT agent for 24 h for surface immobilization. After modification, the Fe_3O_4@SiO_2-CPAD NPs were rinsed with water and dried.

MEMA, CPAD as a free RAFT agent, and AIBN at a molar ratio of 400:5:1 were charged into a Schleck tube containing NPs and NMP. The polymerization solution was degassed with a stream nitrogen and stirred at 70 °C for 18 h to allow for polymerization. After quenching the reaction in liquid nitrogen, the solution was diluted with THF and polymerization solution was then poured into stirred *n*-hexane (87%; $M_{n,SEC}$=11.2 KDa, M_w/M_n=1.25).

2.4 Measurements and Characterization

NMR was performed on a Bruker 300 MHz instrument. Attenuated total reflectance-Fourier transform infrared (FTIR) was performed on a Thermo Nicolet 6700 instrument. The X-ray photoelectron spectra of nanoparticles were recorded by using x-ray photoelectron spectrometer (XPS) (PHI-5000 Versaprobe). Thermogravimetric analysis (TGA) was performed under N_2 atmosphere at a heating rate of 10 °C/min on a Hitachi SII 7300. X-ray diffraction (XRD, Rigaku Ultima IV) was used to determine the crystal structure of the magnetic NPs. A vibrating-sample magnetometer (Cryogenic Limited PPMS) was used at room temperature to measure the magnetic properties of Fe_3O_4 and magnetic composite particles. Transmission electron microscopy (TEM) analysis was performed using JEOL 2010F operating at 200 keV.

3 Results and Discussion

PMEMA-functionalized NPs were prepared as given in Scheme 1. Fe_3O_4 nanoparticles were prepared via a precipitation method than were functionalized with a thin silica layer (Fe_3O_4@SiO_2). In the next step, MNPs were modified with catechol derivative RAFT agent (Fe_3O_4@SiO_2-CPAD). Finally, PMEMA-functionalized NPs were synthesized via RAFT polymerization of

MEMA (Fe_3O_4@SiO_2-PMEMA).

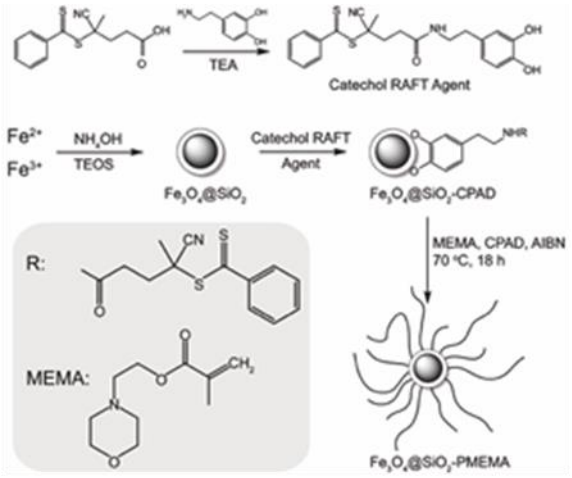

Scheme 1 Schematic illustration of the procedure for preparing PMEMA modified NPs.

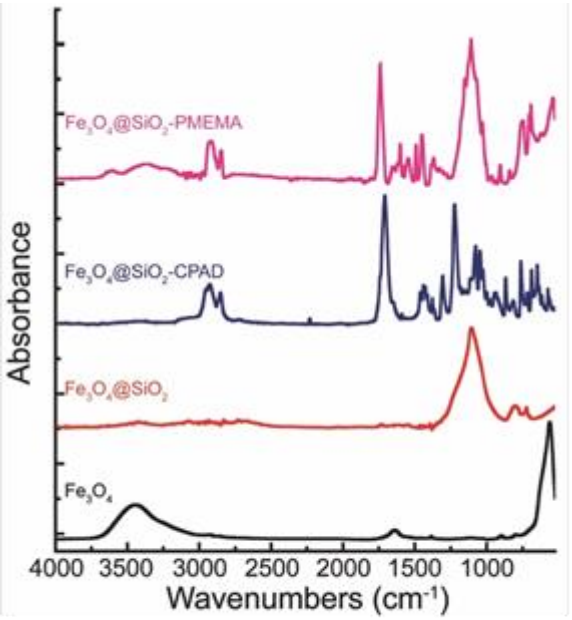

Figure 1 FTIR spectra of pure Fe_3O_4 NPs, Fe_3O_4@SiO_2 NPs, Fe_3O_4@SiO_2-CPAD NPs, and Fe_3O_4@SiO_2-PMEMA NPs.

Figure 1 shows FTIR spectrum of the MNPs. The characteristic band of Fe_3O_4 MNPs (Fe-O-Fe) was observed at 561 cm^{-1}. FTIR spectra of Fe_3O_4@SiO_2 also showed an absorbance band at 1100 cm^{-1} for the Si-O-Si stretching. The peaks at 2950, 2245, 1650, 1550 and 1040 cm^{-1} were assigned to C-H, CN, Amide I (C=O), Amide II (C-N) and C=S stretching of the catechol derivative

RAFT agent modified MNPs, respectively. After RAFT polymerization of the MEMA on MNPs surface, C=O and C-O-C stretching vibration of morpholino monomer at the wavelengths of 1720 and 1100 cm^{-1} were observed.

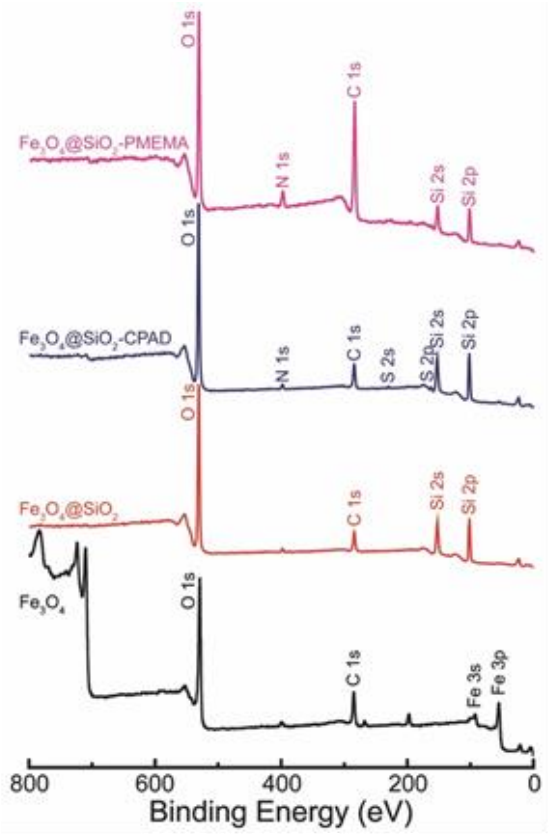

Figure 2 XPS survey scans: pure Fe_3O_4 NPs, Fe_3O_4@SiO_2 NPs, Fe_3O_4@SiO_2-CPAD NPs, and Fe_3O_4@SiO_2-PMEMA NPs.

The chemical nature of the surface coatings was also evidenced by XPS analysis (Figure 2). Fe $2p_{1/2}$ and Fe $2p_{3/2}$ peaks were appeared at 725 and 711 eV, respectively. These two peaks show that, MNPs occurs Fe_3O_4, instead of Fe_2O_3 [32]. XPS analysis of the Fe_3O_4@SiO_2 MNPs verified the presence of Si 2s (153 eV) and Si 2p (103 eV). C 1s XPS peak was observed at near 285 eV for Fe_2O_3 and Fe_3O_4@SiO_2 MNPs. Furthermore, a relatively high amount of oxygen was detected. This was mainly assigned to sample contamination by atmospheric gases and organic dusts [33]. Catechol derivative RAFT agent was confirmed by the appearance of the C 1s (285 eV), N 1s (400 eV), S 2s (233 eV) and S 2p (169 eV) signals. It is showed that RAFT agent was successfully fabricated on Fe_3O_4@SiO_2 MNPs surface. After PMEMA grafting, the carbon and nitrogen signals were increased, whereas silicon and sulfur ratios were decreased in the XPS spectra. Successful immobilization of PMEMA on MNPs surface was investigated by FTIR and XPS analysis.

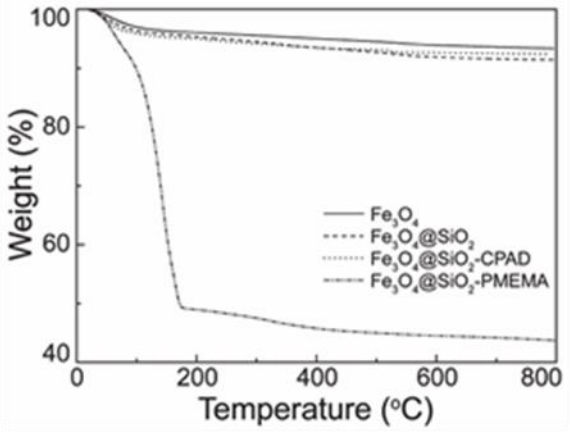

Figure 3 TGA thermograms of pure Fe_3O_4 NPs, Fe_3O_4@SiO_2 NPs, Fe_3O_4@SiO_2-CPAD NPs, and Fe_3O_4@SiO_2-PMEMA NPs.

The amount of organic content at the MNPs surface was determined from the TGA analysis (Figure 3). It can be seen that about 6.68wt%, 8.53wt%, 56.23wt% of weight loss at 800 °C for Fe_3O_4@SiO_2, Fe_3O_4@SiO_2-CPAD MNPs and Fe_3O_4@SiO_2-PMEMA MNPs, respectively. To compare the samples of Fe_3O_4@SiO_2-PMEMA and Fe_3O_4@SiO_2-CPAD, the grafting amount of PMEMA could be calculated as 45 mg/g. This result confirms again the successful immobilization of PMEMA on Fe_3O_4@SiO_2-CPAD NPs surface.

The X-ray diffraction (XRD) patterns of unmodified and modified NPs are depicted in Figure 4. For bare Fe_3O_4, the main peaks centered at 2θ = 30°, 35°, 43°, 53°, 57°, and 62°, which corresponded to (220), (311), (400), (422), (511), and (440), respectively. All the peak positions were basically consistent with the standard data for Fe_3O_4 structure (JCPDS file No. 85-1436). The broad peak appeared in the range from 18 to 28 indicates the existence of amorphous PMEMA. It was found that the main peaks of Fe_3O_4@SiO_2-PMEMA coincide with those of unmodified Fe_3O_4. The XRD results suggest that the modification via combination of grafting from and RAFT polymerization did not change the crystalline structure of Fe_3O_4 nanoparticles.

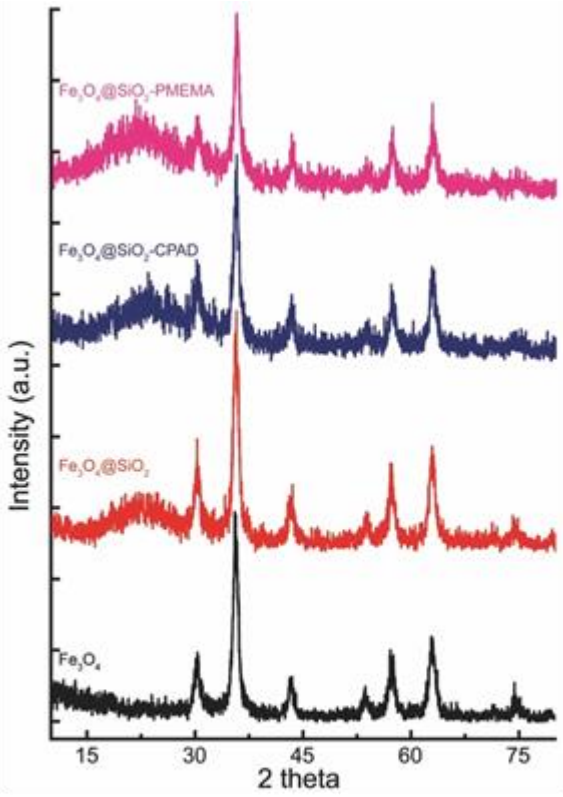

Figure 4 XRD patterns of Fe_3O_4 NPs, Fe_3O_4@SiO_2 NPs, Fe_3O_4@SiO_2-CPAD NPs, and Fe_3O_4@SiO_2-PMEMA NPs.

The magnetic properties of unmodified and modified MNPs were recorded using a VSM at 300 K as shown in magnetization curves in Figure 5. The magnetization curves clearly point out a difference in the magnetic properties of MNPs. The Fe_3O_4, Fe_3O_4@SiO_2, Fe_3O_4@SiO_2-CPAD and Fe_3O_4@SiO_2-PMEMA have saturation magnetization values of 56.6, 31.5, 30.8 and 15.7 emu/g, respectively. The bare Fe_3O_4 showed the highest magnetization. However, it was decreased after the surface functionalization, because of the thick shell surrounding the magnetic cores. However, these results showed that Fe_3O_4@SiO_2-PMEMA NPs have a strong magnetic response to an applied magnetic field.

The prepared NPs were analyzed by TEM. Figure 6 showed representative images of the NPs. The aggregation of the nanoparticles arises because of the evaporation of the solvent. The mean diameter of bare Fe_3O_4 nanoparticles is about 10 nm. Particle size didn't change much from Figure 6a to c. The dark Fe_3O_4@SiO_2 NPs were coated by a hazy PMEMA layer with a thickness of about 25 nm. The Fe_3O_4@SiO_2-PMEMA NPs which have a core/shell structure were easily prepared from a biomimetic RAFT agent com-

pared with the previously published studies [34-36].

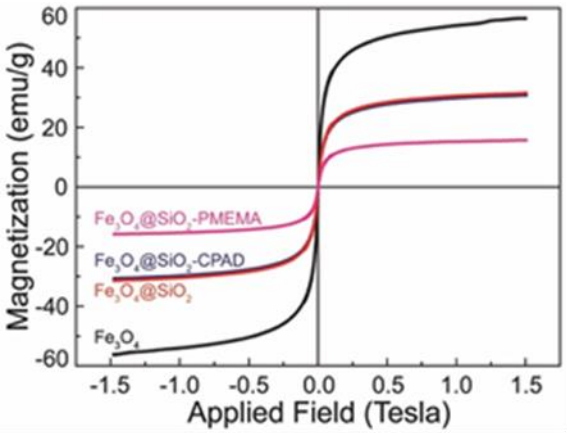

Figure 5 Magnetic hysteresis loops for the pure Fe_3O_4 NPs, Fe_3O_4@SiO_2 NPs, Fe_3O_4@SiO_2-CPAD NPs, and Fe_3O_4@SiO_2-PMEMA NPs.

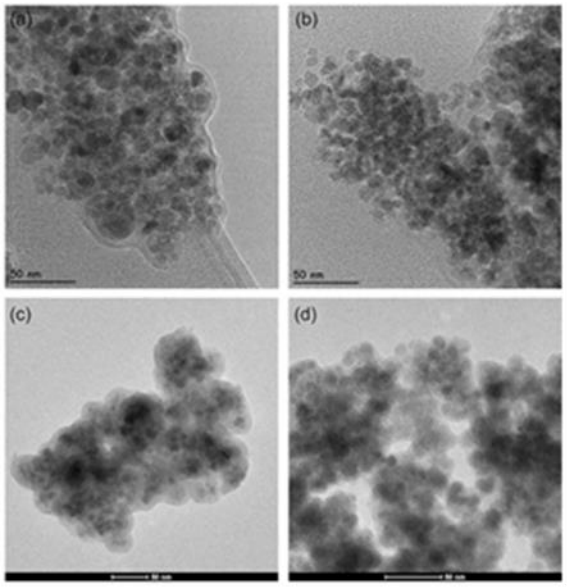

Figure 6 TEM images of the (a) pure Fe_3O_4 NPs, (b) Fe_3O_4@SiO_2 NPs, (c) Fe_3O_4@SiO_2-CPAD NPs, and (d) Fe_3O_4@SiO_2-PMEMA NPs.

4 Conclusions

In conclusion, functional NPs were successfully prepared via surface initiated RAFT polymerization from a biomimetic RAFT agent. Fe_3O_4 NPs were prepared and then embedded by a silica layer. Catechol derivative RAFT agent was immobilized on the Fe_3O_4@SiO_2 surface. RAFT agent immobilized Fe_3O_4@SiO_2 NPs were used to mediate homopolymerization of MEMA. The modification steps of Fe_3O_4@SiO_2 NPs were confirmed by FTIR, XPS, XRD, TGA and TEM analysis. It is suggested that surface initiated RAFT polymerization from catechol-based biomimetic RAFT agent surface would be a promising strategy to prepare functional materials. Our future work will focus on the preparation and application of the stimuli responsive polymer coated NPs via biomimetic surface modification methods, with the goal of creating smart biomaterials.

Acknowledgements

This work was partially supported by the Scientific and Technological Research Council of Turkey - TÜBİTAK (project#112T868), and Scientific Research Projects Coordination Unit of Amasya University (project#FMB-BAP 13-023). The authors also thank to the METU Central Lab. (MerLab) and Amasya University Central Research Lab. (AUMAULab) for the use of facilities.

5 References

[1] Andhariya, N.; Chudasama, B.; Mehta, R.V.; Upadhyay, R.V. Biodegradable thermoresponsive polymeric magnetic nanoparticles: a new drug delivery platform for doxorubicin. J. Nanopart. Res. 2011; 13, 1677-1688.

[2] Gu, H.; Xu, K.; Xu, C.; Xu, B. Biofunctional magnetic nanoparticles for protein separation and pathogen detection. Chem. Commun. 2006; 2006, 941-949.

[3] Gupta, A. K.; Gupta, M. Synthesis and surface engineering of iron oxide nanoparticles for biomedical applications. Biomaterials 2005; 26, 3995-4021.

[4] Liong, M.; Lu, J.; Kovochich, M.; Xia, T.; Ruehm, S.G.; Nel, A.E.; Tamanoi, F.; Zink, J.I. Multifunctional inorganic nanoparticles for imaging, targeting, and drug delivery. ACS Nano 2008; 2, 889-896.

[5] Mornet, S.; Vasseur, S.; Grasset, F.; Duguet, E. Magnetic nanoparticle design for medical diagnosis and therapy. J. Mater. Chem. 2004; 14, 2161-2175.

[6] Qiang, Y.; Antony, J.; Sharma, A.; Nutting, J.; Sikes, D.; Meyer, D. Iron/iron oxide core-shell nanoclusters for biomedical applications. J. Nanopart. Res. 2006; 8, 489-496.

[7] Shubayev, V.I.; Pisanic, II T.R.; Jin, S. Magnetic nanoparticles for theragnostics. Adv. Drug. Deliver. Rev. 2009; 61, 467-477.

[8] Uzuriaga-Sánchez, R.J.; Khan, S.; Wong, A.; Picasso, G.; Pividori, M.I.; Sotomayor, M.D.P.T. Magnetically separable polymer (Mag-MIP) for selective analysis of biotin in food samples. Food Chem. 2016; 190, 460-467.

[9] Lu, L.; Li, J.; Yu, J.; Song, P.; Ng, D.H.L. A hierarchically porous $MgFe_2O_4$/γ-Fe_2O_3 magnetic microspheres for efficient removals of dye and pharmaceutical from water. Chemical Eng. Journal 2016; 283, 524-534.

[10] Sheiko, S.S.; Sumerlin, B.S.; Matyjaszewski, K. Cylindrical molecular brushes: Synthesis, characterization, and properties. Prog. Polym. Sci. 2008; 33, 759-785.

[11] Zhang, M.; Breiner, T.; Mori, H.; Müller, A.H.E. Magnetically separable polymer (Mag-MIP) for selective analysis of biotin in food samples. Polymer 2003; 44, 1449-1458.

[12] Zhao, B.; Brittain, W.J. Polymer brushes: surface-immobilized macromolecules. Prog. Polym. Sci. 2000; 25, 677-710.

[13] Cimen, D.; Caykara, T. Preparation of oligo-*N*-isopropylacrylamide brushes with -OH and -COOH end-groups via surface-initiated NMP. J. Appl. Polym. Sci. 2013; 129, 383-390.

[14] Demirci, S.; Kinali-Demirci, S.; Caykara, T. Stimuli-responsive diblock copolymer brushes via combination of "click chemistry" and living radical polymerization. J. Polym. Sci. Part A: Polym. Chem. 2013; 51, 2677-2685.

[15] Boyes, S.G.; Brittain, W.J.; Weng, X.; Cheng, S.Z.D. Synthesis, characterization, and properties of aba type triblock copolymer brushes of styrene and methyl acrylate prepared by atom transfer radical polymerization. Macromolecules 2002; 35, 4960-4967.

[16] Baskaran, D.; Mays, J.W.; Bratcher, M.S. Polymer-grafted multiwalled carbon nanotubes through surface-initiated polymerization. Angew. Chemie. 2004; 43, 2138-2142.

[17] Demirci, S.; Caykara, T. RAFT-mediated synthesis of cationic poly[(ar-vinylbenzyl)trimethyl ammonium chloride] brushes for quantitative DNA immobilization. Mater. Sci. Eng. C Mater. Biol. Appl. 2013; 33; 111-120.

[18] Rungta, A.; Natarajan, B.; Neely, T.; Dukes, D.; Schadler, L. S.; Benicewicz, B.C. Grafting bimodal polymer brushes on nanoparticles using controlled radical polymerization. Macromolecules 2012; 45, 9303-9311.

[19] Demirci, S.; Caykara, T. High density cationic polymer brushes from combined "click chemistry" and RAFT-mediated polymerization. J. Polym. Sci. Part A: Polym. Chem. 2012; 50, 2999-3007.

[20] Demirci, S.; Caykara, T. Controlled grafting of cationic poly[(ar-vinylbenzyl)trimethylammonium chloride] on hydrogen-terminated silicon substrate by surface-initiated RAFT polymerization. React. Funct. Polym. 2012; 72, 588-595.

[21] Baum, M.; Brittain, W.J. Synthesis of polymer brushes on silicate substrates via reversible addition fragmentation chain transfer technique. Macromolecules 2002; 35, 610-615.

[22] Zhai, G.; Yu, W.H.; Kang, E.T.; Neoh, K.G.; Huang, C. C.; Liaw, D. Magnetically separable polymer (Mag-MIP) for selective analysis of biotin in food samples. J. Ind. Eng. Chem. Res. 2004; 43, 1673-1680.

[23] Demirci, S.; Kinali-Demirci, S.; Caykara, T. A new selenium-based RAFT agent for surface-initiated RAFT polymerization of 4-vinylpyridine. Polymer 2013; 54, 5345-5350.

[24] Li, C.; Han, J.; Ryu, C. Y.; Benicewicz, B.C. A versatile method to prepare RAFT agent anchored substrates and the preparation of PMMA grafted nanoparticles. Macromolecules 2006; 39, 3175-3183.

[25] Li, C.; Benicewicz, B.C. Synthesis of well-defined polymer brushes grafted onto silica nanoparticles via surface reversible addition−fragmentation chain transfer polymerization. Macromlecules 2005; 38, 5929-5936.

[26] Tria, M.C.R.; Grande, C.D.T.; Ponnapati, R.R.; Advincula, R.C. Electrochemical deposition and surface-initiated raft polymerization: protein and cell-resistant ppegmema polymer brushes. Biomacromolecules 2010; 11, 3422-3431.

[27] Gurbuz, N.; Demirci, S.; Yavuz, S.; Caykara, T. Synthesis of cationic *N*-[3-(dimethylamino)propyl] methacrylamide brushes on silicon wafer via surface-initiated RAFT polymerization. J. Polym. Sci. Part A: Polym. Chem. 2011; 49, 423-431.

[28] Liu, J.; Li, J.; Yu, B.; Ma, B.; Zhu, Y.; Song, X.; Cao, X.; Yang, W.; Zhou, F. Tribological properties of self-assembled monolayers of catecholic imidazolium and the spin-coated films of ionic liquids. Langmuir 2011; 27, 11324-11331.

[29] Liu, J.; Yang, W.; Zareie, H.M.; Gooding, J.J.; Davis, T. P. pH-detachable polymer brushes formed using titanium-diol coordination chemistry and living radical polymerization (RAFT). Macromolecules 2009; 42, 2931-2939.

[30] Zobrist, C.; Sobocinski, J.; Lyskawa, J.; Fournier, D.; Miri, V.; Traisnel, M.; Jimendez, M.; Woisel, P. Functionalization of titanium surfaces with polymer brushes prepared from a biomimetic RAFT agent. Macromolecules 2011; 44, 5883-5892.

[31] Ranjbakhsh, E.; Bordbar, A.K.; Abbasi, M.; Khosropour, A.R.; Shams, E. Enhancement of stability and catalytic activity of immobilized lipase on silica-coated modified magnetite nanoparticles. Chemical Eng. Journal 2012; 179, 272-276.

[32] Farrukh, A.; Akram, A.; Ghaffar, A.; Hanif, S.; Hamid, A.; Duran, H.; Yameen, B. Design of polymer-brush-grafted magnetic nanoparticles for highly efficient water remediation. ACS Appl. Mater. Interfaces 2013; 5, 3784-3793.

[33] Satyanarayana, N.; Sinha, S.K. Tribology of PFPE overcoated self-assembled monolayers deposited on Si surface. J. Phys. D: Appl. Phys. 2005; 38, 3512-3522.

[34] Jiang, X.; Zhai, S.; Jiang, X.; Lu, G.; Huang, X. Synthesis of PAA-g-PNIPAM well-defined graft polymer by sequential RAFT and SET-LRP and its application in preparing size-controlled super-paramagnetic Fe_3O_4 nanoparticles as a stabilizer. Polymer 2014; 55, 3703-3712.

[35] Li, Q.; Zhang, L.; Bai, L.; Zhang, Z.; Zhu, J.; Zhou, N.; Cheng, Z.; Zhu, X. Multistimuli-responsive hybrid nanoparticles with magnetic core and thermoresponsive fluorescence-labeled shell via surface-initiated RAFT polymerization. Soft Matter 2011; 7, 6958-6966.

[36] Wu, Y.; Yang, H.; Lin, Y.; Zheng, Z.; Ding, X. Poly(N-isopropylacrylamide) modified Fe3O4@Au nanoparticles with magnetic and temperature responsive properties. Mater. Lett. 2016; 169, 218-222.